ACS Medicinal Chemistry Letters

Letter

pubs.acs.org/acsmedchemlett

A Fluorescent Styrylquinoline with Combined Therapeutic and Diagnostic Activities against Alzheimer's and Prion Diseases

Matteo Staderini,[†] Suzana Aulić,[‡] Manuela Bartolini,[§] Hoang Ngoc Ai Tran,[‡] Víctor González-Ruiz,[∥] Daniel I. Pérez,[⊥] Nieves Cabezas,[†] Ana Martínez,[⊥] M. Antonia Martín,[∥] Vincenza Andrisano,[§] Giuseppe Legname,[‡] J. Carlos Menéndez,[†] and Maria Laura Bolognesi*[,§]

[†]Departamento de Química Orgánica y Farmacéutica and [∥]Sección Departamental de Química Analítica, Facultad de Farmacia, Universidad Complutense, 28040 Madrid, Spain

[‡]SISSA, Neuroscience Department, Via Bonomea 265, 34136 Trieste, Italy

[§]Department of Pharmacy and Biotechnology, Alma Mater Studiorum, University of Bologna, Via Belmeloro 6, 40126 Bologna, Italy

[⊥]Instituto de Química Médica-CSIC, Juan de la Cierva 3, 28006 Madrid, Spain

Supporting Information

ABSTRACT: (*E*)-6-Methyl-4′-amino-2-styrylquinoline (**3**) is a small molecule with the proper features to potentially diagnose, deliver therapy and monitor response to therapy in protein misfolding diseases. These features include compound fluorescent emission in the NIR region and its ability to interact with both Aβ and prion fibrils, staining them with high selectivity. Styrylquinoline **3** also inhibits Aβ self-aggregation in vitro and prion replication in the submicromolar range in a cellular context. Furthermore, it is not toxic and is able to cross the blood brain barrier in vitro (PAMPA test).

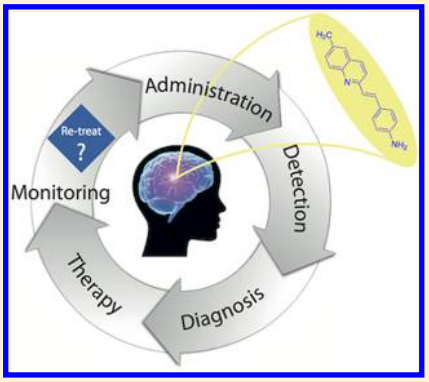

KEYWORDS: *Aggregation, protein misfolding diseases, amyloid, fibrillation inhibitors*

Protein misfolding diseases (PMD) include a broad range of human disorders characterized by a conformational change of normally expressed proteins, that convert from a physiological soluble monomeric form into oligomeric and fibrillar forms, rich in stable β-sheet regions.[1] These fibrillar aggregates play a pivotal role in neuronal dysfunction and survival, eventually leading to fatal disease. Alzheimer's (AD) and prion diseases (PrD) are prototypical examples of PMD. In these maladies, amyloid-β protein (Aβ) and cellular prion protein (PrP^{C}), respectively, change their conformations into β-sheet toxic isoforms. In the case of PrD, the toxic isoform known as scrapie prion protein (PrP^{Sc}) is also infectious.[2]

In AD and PrD, the misfolded proteins have been regarded both as neuropathological hallmarks for diagnosis and as therapeutic targets.[2] While the so-called "amyloid hypothesis" in AD has been questioned, a recent interest has arisen in the possibility that all proteins causing neurodegeneration are prions.[2] If confirmed, this hypothesis would profoundly influence the development of diagnostic and therapeutic tools.[2]

Many techniques have been employed to detect fibrillar aggregates, including positron emission tomography (PET)[3] and fluorescence spectroscopy.[4] PET is expensive and limited by the narrow isotope availability of the required probes. On the other hand, many fluorescent in vitro staining agents are available such as Congo Red (CR) and Thioflavin T (ThT) but they cannot translate into clinical diagnostic and therapeutic tools[4] because of their low specificity, poor sensitivity, inability to cross the blood brain barrier (BBB) and marked toxicity.[5] Because fluorescence spectroscopy has proven suitable for studying fibrillar aggregates also in vivo,[6−9] there is an urgent need for fluorescent sensors with improved properties.

With these concepts in mind, we focused our attention on fluorescent compounds capable of staining Aβ and PrP^{Sc} fibrils and, ideally, of simultaneously blocking their aggregation. To this aim, ideal properties for a therapeutic and diagnostic small molecule should include (1) ability to change fluorescence properties upon binding to fibrils, (2) ability to absorb and emit light in the far red/near-infrared (NIR) region (ca. 600−800 nm),[7] where tissue scattering and absorption is lowest,[10] (3) large Stokes shift, (4) ability to modulate fibril aggregation, (5) minimum interference from human serum albumin (HSA) binding, (6) a small molecular size, which enables the small molecule to cross the BBB, and (7) low toxicity.[6−9,11]

Received: October 22, 2012
Accepted: December 27, 2012
Published: December 28, 2012

   dx.doi.org/10.1021/ml3003605 | *ACS Med. Chem. Lett.* 2013, 4, 225−229

As a starting point, we noticed that several styryl derivatives, designed by Li et al. to improve the pharmacokinetic properties of CR and ThT, were employed as AD imaging agents in vivo.[12] Interestingly, some of them were also found to be active against prion replication in infected cells.[13] Furthermore, Ishikawa et al. reported that a styrylbenzene derivative (BSB) was useful to detect PrP^{Sc} aggregates ex vivo and showed effectiveness in cellular assays.[14] An isolated example of an (*o*-hydroxystyryl)quinoline was described as a binder of both amyloid and prion fibrils,[15] and, very recently, Yang et al. reported styryl-1*H*-indole and styrylquinoline derivatives as SPECT imaging probe to detect Aβ plaques.[16] These literature data show that the styryl moiety is critical to the ability of small molecules to label and interfere with pathological fibrillar aggregates, in both PrD and AD.

Here we report a preliminary exploration of styrylquinolines **1**−**3** as Aβ/PrP^{Sc} diagnostic and therapeutic small molecules. We focused on a quinoline moiety because it constitutes the core of many antiprion compounds (i.e., chloroquine and mefloquine),[17] while displaying good pharmacokinetic properties and a high degree of druglikeness. An amino group was purposely introduced (**3**) to have an electron-releasing substituent conjugated with the quinoline nitrogen to shift the fluorescence emission toward the far red/NIR spectral region. In order to reinforce this effect by increasing the electron-withdrawing character of the quinoline nitrogen, the hydrochloride salt of **3** was also prepared.

Compounds **1** and **2** were synthesized via a vinylogous variation of the Povarov reaction,[18] while the amino derivative **3** was prepared by treating **1** with a mixture of fuming and concentrated nitric acids followed by reduction of the crude nitration product with iron powder in concentrated HCl. This protocol afforded **3** in 68% yield after chromatography, together with a small amount of the corresponding ortho derivative (Scheme 1).

Scheme 1. Synthesis of Styrylquinolines 1−3[a]

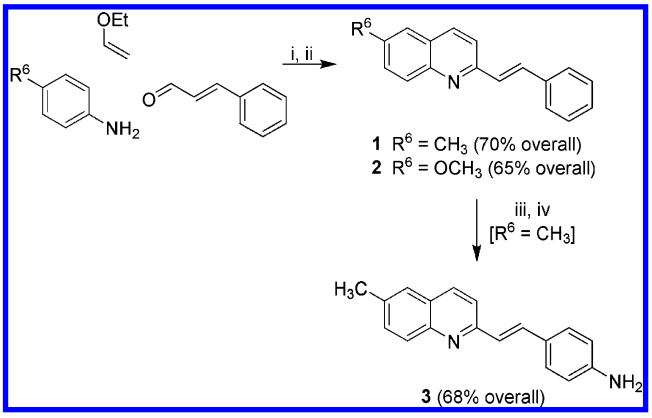

[a]Reagents and conditions: (i) CAN (15%), CH_3CN, rt, 5 h; (ii) DDQ, benzene, rt, 3 h; (iii) 65% HNO_3/fuming HNO_3 (2:8), rt, 14 h.; (iv) Fe, 38% HCl, AcOH, EtOH, reflux, 4 h.

We first investigated the native fluorescence of styrylquinolines **1**−**3** in several solvents, including phosphate buffered saline (PBS) at physiological pH. In the case of **3**, the fluorescence emission greatly depended on solvent polarity (Figure 1A,B and Tables S1 and S2 in the Supporting Information). Its fluorescence emission in ethanol—whose polarity mimics the protein environment—was red-shifted with

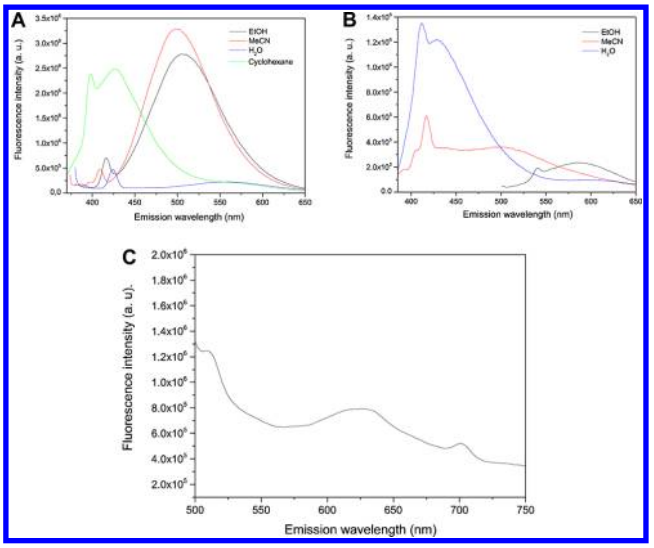

Figure 1. Fluorescence spectra for **3** (A) and **3**·HCl (B) in solution, and for **3**·HCl in the solid state (C).

regard to the more polar water solvent. Since compound **3** would be adsorbed onto protein aggregates where its free movement would be restricted, the fluorescence emission of **3**·HCl in the solid state was also obtained (Figure 1C). Interestingly, an emission maximum above 600 nm was observed. On this basis we consider **3** as a starting lead compound which can be easily manipulated by increasing the electron-donating/accepting ability of the molecule to enhance the spectral bathochromic shift, facilitating its use of this compound as a NIR sensor.[19] An additional advantageous feature of **3** is its large Stokes shift (>150 nm), which minimizes interference from the exciting radiation (Tables S1 and S2 in the Supporting Information).

To assess the potential value of our compounds as CNS-directed agents, the capability of **1**−**3** to cross the BBB was studied by the parallel artificial membrane permeability assay (PAMPA).[20] Experimental data allowed us to predict optimal BBB permeation for **2** and **3** (Table 1).

In vitro activities of compounds **1**−**3** on the target proteins were then investigated. The inhibitory potency of **1**−**3** as antiaggregating agents toward Aβ_{42} was determined by a ThT-based fluorometric assay.[21] When tested at a 1:1 ratio with Aβ_{42}, **1** and **2** did not significantly alter amyloid fibril formation,

Table 1. In Vitro Permeability (Pe) Values[a] with Related Predictive Penetration into the CNS[b] and Antiprion Activity and Cell Viability of 1−3 on ScGT1 Cells[c]

compd	Pe (10^{-6} cm s^{-1})[a]	prediction[b]	EC_{50} (μM)[d]	% of viable cells at EC_{50}[d]
quinacrine			0.4 ± 0.1	100.0 ± 4.3
GN8			1.5 ± 0.1	93.4 ± 7.3
1	3.0 ± 0.6	CNS +/−	0.5 ± 0.1	90.5 ± 6.8
2	8.5 + 1.1	CNS +	0.7 ± 0.1	74.9 ± 4.1
3	23.1 ± 1.9	CNS +	0.5 ± 0.1	94.6 ± 4.9

[a]Mean ± standard deviation (SD) of two experiments. [b]CNS + means Pe > 3.74 × 10^{-6} cm s^{-1}, and CNS ± means Pe between 3.74 × 10^{-6} and 1.50 × 10^{-6} cm s^{-1}. [c]Mean ± SD of three experiments. [d]Effect of **1**−**3** on inhibition of PrP^{Sc} replication and cell viability was measured as reported in ref 25. Full details of the biological methods are given in the Supporting Information.

dx.doi.org/10.1021/ml3003605 | *ACS Med. Chem. Lett.* 2013, 4, 225−229

while **3** decreased the fluorescence signal by 42.4 ± 2.6%, thus behaving as an inhibitor of fibrilization and an amyloid binder. On the basis of data available in the literature, **3** can be ranked as a moderate inhibitor, with potency slightly lower than that of the well-known antiaggregating compound curcumin,[22] which, in the same assay conditions, was able to inhibit fibril formation by 73%. No negative or positive interference in the fluorescence signal of ThT was observed under the experimental conditions (see Supporting Information and Figure 2C). In the light of these findings, compound **3** was regarded sufficiently interesting to warrant further study.

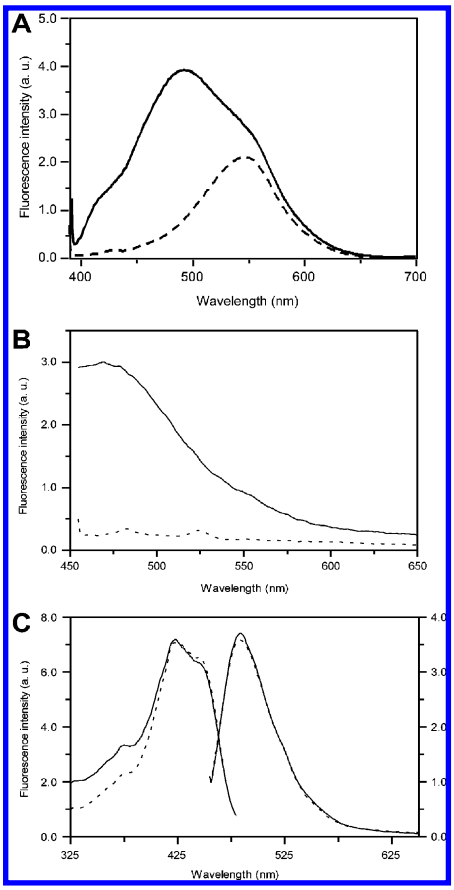

Figure 2. (A) Fluorescence emission spectra of **3** (5 μM) in aqueous phosphate buffer (10 mM, pH 7.4) in the absence (dotted line) and in the presence (solid line) of aggregated Aβ_{42} (3 μM). (B) Fluorescence emission spectra of a solution containing aggregated Aβ_{42} protein and **3** [25 nM] in glycine−NaOH buffer (50 mM, pH 8.5) recorded at the excitation maximum of ThT (λ_{ex} = 446 nm, dotted line) and at the excitation maximum of **3** (λ_{exc} = 375 nm, solid line). (C) Excitation (λ_{em} = 490 nm) and emission (λ_{exc} = 446 nm) spectra of a solution containing aggregated Aβ_{42} protein in 1.5 μM ThT buffered solution (glycine−NaOH buffer, 50 mM pH 8.5) in the presence (dotted line) and absence (solid line) of **3** [25 nM].

Due to its potential application as an amyloid sensor, the emission spectra of compound **3** in the absence and presence of aggregated Aβ_{42} were recorded. While the excitation maxima for the bound and unbound forms of **3** did not significantly differ, a strong hypsochromic shift of the emission maximum (from 528 to 490 nm), concomitant with a hyperchromic effect upon binding, was observed (Figure 2A). In agreement with studies in solvents with decreasing polarity, this behavior seems related to a change in the environmental conditions, as the binding of **3** to the amyloid fibrils places it in a lower dielectric constant environment. Indeed, adopting the β-sheet secondary structure in the Aβ_{42} self-assembly process is likely to expose hydrophobic regions that are accessible to **3**. The spectral shift observed for **3** is similar to that reported for the Aβ_{42} fluorescent sensor 1-anilinophthalene-8-sulfonic acid.[23] Furthermore, the fluorescence emission intensity at 450 nm linearly correlated with the concentration of preaggregated Aβ_{42} (R^2 = 0.9992) (Figure S1 in the Supporting Information).

Finally, to gain further insights into the binding mode of **3** to Aβ, displacement studies in the presence of aggregated Aβ_{42} were carried out using a fixed concentration of Aβ_{42} and ThT and an increasing concentration of **3**. Overlaid excitation spectra show that **3** binds amyloid fibrils with a high affinity. At a low concentration (25 nM) and in the presence of Aβ_{42}, **3** shows a significant emission signal (Figure 2B) without affecting the ThT excitation and emission profile (Figure 2C). Conversely, at higher concentrations, **3** progressively displaces ThT from its binding site(s)[24] (Figure S2 in the Supporting Information). This led us to hypothesize that **3** may have a primary high affinity binding site distinct from ThT and a secondary low-affinity binding site in common with ThT. To discard the interference of HSA, a comparison between the changes in the fluorescence intensity in the presence of HSA and Aβ_{42} was carried out. It evidenced a stronger fluorescence change for the latter peptide, as deduced from the slopes of the titration plots (Figure S3 in the Supporting Information).

In addition, the capability to inhibit prion fibril formation in vitro was studied, using a known amyloid seeding assay (ASA).[25] At a concentration of 50 μM, **1**−**3** delayed fibril formation, extending the lag phase to ≥70 h (control: 59 h) (Figure S4 in the Supporting Information). A similar profile was found for GN8, an antiprion drug candidate, for which a specific binding with PrP has been experimentally demonstrated.[26]

Taken together, these results show that our candidate molecule **3** is indeed able to recognize, stain and modulate Aβ_{42} and PrP^{Sc} fibril aggregation in vitro.

Next, the therapeutic antiprion potential (toxicity and activity) of **1**−**3** was preliminarily assessed in a cell-based model of PrD (ScGT1 cells). At a 1 μM concentration, **1** and **3** showed a very low toxicity, with cell viability above 90%, while **2** caused viability to decrease to 60%. Interestingly, at a 10 μM concentration **3** still showed a tolerable toxicity, with a residual 60% cell viability not different from that of drug candidate GN8 (Figure S5 in the Supporting Information).

The three compounds were studied for their antiprion activity in a nontoxic range of concentrations (Table 1). They all showed remarkable activities (submicromolar EC_{50} values), which make them more potent than GN8 and equipotent to the gold standard quinacrine. Cell viability at the concentration corresponding to EC_{50} was particularly high for **3** (94.6%).

To confirm the labeling of PrP^{Sc} aggregates in living cells, fluorescent staining with **3** was carried out using the same ScGT1 cell model (Figure 4). To corroborate the data an additional cell line (ScN2a) was used (Figures S11−S15 in the Supporting Information). We found that 0.025% of **3**·HCl (0.84 mM) was sufficient to observe many fluorescent spots in the treated cells examined by fluorescent microscopy (Figure 3A,B). Importantly, no spots were observed in the uninfected cells (Figure 3D−F), confirming a specific binding. Furthermore, the staining pattern was consistent with that observed with 0.025% Thioflavin S (ThS), a common PrP^{Sc} dye (Figures

dx.doi.org/10.1021/ml3003605 | ACS Med. Chem. Lett. 2013, 4, 225−229

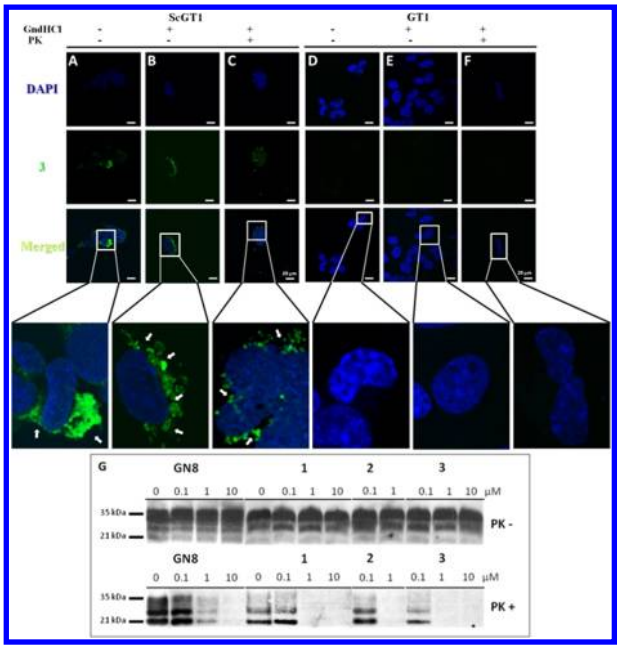

Figure 3. Detection of PrP^{Sc} aggregates with **3**·HCl in ScGT1 cells by intensity fluorescence (IF) before (A) and after (B) denaturation with 6 M guanidinium chloride (GndHCl). After PK digestion, PK resistant PrP (PrP^{Sc}) was observed with **3**·HCl (C). Uninfected GT1 cells with or without denaturation step with 6 M GndHCl (D, E) and after PK digestion (F) did not show staining in the presence of **3**·HCl (0.84 mM). (G) Dose-dependent capacity of **1**, **2** and **3** to decrease PrP^{Sc} levels in comparison with GN8. Western blotting of ScGT1 cell lysates depicting the presence or absence of prions (PrP^{Sc}) following treatment with GN8 and **1**, **2**, **3** before (top) or after (bottom) PK digestion.

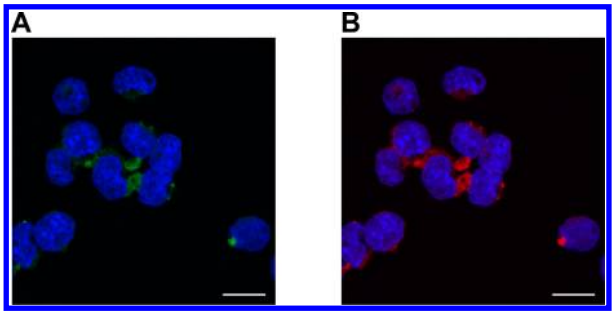

Figure 4. ScGT1 cell line treated with 6 M GndHCl and stained with compound **3**. (A) FITC filter. (B) ThS filter. Nuclei stained with DAPI (blue). Scale bar 20 μm.

S8 and S12 in the Supporting Information). A further experiment proved that **3**·HCl (0.25 mM) distinguishes the abnormal, aggregated and proteinase K (PK) resistant PrP^{Sc} isoform from the normal, PK-sensitive PrP^{C} isoform. Thus, after eliminating PrP^{C} through a PK digestion step, the previous fluorescence-staining pattern was observed (Figure 3C). We primarily used the FITC filter set for these studies, but we confirmed the staining by employing the ThS one, which is within the NIR optical window (Figure 4). At these emission wavelengths, no interference from HSA was observed (Figure S3 in the Supporting Information).

In summary, we have obtained considerable evidence that **3** is potentially useful to diagnose, deliver targeted therapy and monitor response to therapy in PMD. Indeed, from a medicinal chemistry perspective **3** offers peculiar advantages: (1) a lower molecular weight than previous sensors,[19] (2) a small-molecule scaffold which is easily amenable to further manipulation to improve fluorescence response and amyloid-binding properties. Most importantly, with respect to the previously reported NIR amyloid sensors,[6−9,11] it offers the additional advantage of a concomitant promising antifibrillar profile (in vitro and in a cellular context), together with a low toxicity. If these peculiar properties are confirmed in vivo, **3** is likely to become the first purposely designed therapeutic and diagnostic tool (theranostic) for PrD and AD.

■ ASSOCIATED CONTENT

Ⓢ Supporting Information

Spectra, biological assay data and experimental procedures. This material is available free of charge via the Internet at http://pubs.acs.org.

■ AUTHOR INFORMATION

Corresponding Author

*Phone: +39 051 209 9718. Fax: +39 051 209 9734. E-mail: marialaura.bolognesi@unibo.it.

Author Contributions

M.S. and S.A. contributed equally to this research. The manuscript was written through contributions of all authors. All authors have given approval to the final version of the manuscript.

Funding

Financial support from MICINN (Grants CTQ2009-12320-BQU and SAF2009-13015-C02-01), UCM (Grupos de Investigación, Grant GR35/10-A-920234), Ministero dell'Istruzione, dell'Università e della Ricerca under the program PRIN 2008 (Meccanismi Neurodegenerativi nelle Malattie da Prioni: Studi Conformazionali, Fisiopatologia della Proteina Prionica e Possibili Approcci Farmacologici), PRIN 2009 and PRIN 2010 is gratefully acknowledged. D.I.P. acknowledges a postdoctoral fellowship from CSIC (JAE program).

Notes

The authors declare no competing financial interest.

■ ABBREVIATIONS

PMD, protein misfolding diseases; AD, Alzheimer's disease; PrD, prion diseases; Pr^{C}, Pr^{Sc}, cellular and scrapie prion protein; PBS, phosphate buffer saline; HSA, human serum albumin; PET, positron emission tomography; CR, Congo Red; ThT, Th S, Thioflavin T and S; BBB, blood brain barrier; NIR, near-infrared; PAMPA, parallel artificial membrane permeability assay; ASA, amyloid seeding assay; PK, proteinase K; GndHCl, guanidium chloride; IF, intensity fluorescence

■ REFERENCES

(1) Chiti, F.; Dobson, C. M. Protein misfolding, functional amyloid and human disease. *Annu. Rev. Biochem.* **2006**, *75*, 333−366.

(2) Prusiner, S. B. A unifying role for prions in neurodegenerative diseases. *Science* **2012**, *336*, 1511−1513.

(3) Kung, H. F. The β-amyloid hypothesis in Alzheimer's disease: seeing is believing. *ACS Med. Chem. Lett.* **2012**, *3*, 265−267.

(4) Bertoncini, C. W.; Celej, M. S. Small molecule fluorescent probes for the detection of amyloid self-assembly in vitro and in vivo. *Curr. Protein Pept. Sci.* **2011**, *12*, 206−220.

(5) Hong, Y.; Meng, L.; Chen, S.; Leung, C. W.; Da, L. T.; Faisal, M.; Silva, D. A.; Liu, J.; Lam, J. W.; Huang, X.; Tang, B. Z. Monitoring and inhibition of insulin fibrillation by a small organic fluorogen with

aggregation-induced emission characteristics. *J. Am. Chem. Soc.* **2012**, *134*, 1680−1689.
(6) Hintersteiner, M.; Enz, A.; Frey, P.; Jaton, A. L.; Kinzy, W.; Kneuer, R.; Neumann, U.; Rudin, M.; Staufenbiel, M.; Stoeckli, M.; Wiederhold, K. H.; Gremlich, H. U. In vivo detection of amyloid-beta deposits by near-infrared imaging using an oxazine-derivative probe. *Nat. Biotechnol.* **2005**, *23*, 577−583.
(7) Nesterov, E. E.; Skoch, J.; Hyman, B. T.; Klunk, W. E.; Bacskai, B. J.; Swager, T. M. In vivo optical imaging of amyloid aggregates in brain: design of fluorescent markers. *Angew. Chem. Int. Ed.* **2005**, *44*, 5452−5456.
(8) Ran, C.; Xu, X.; Raymond, S. B.; Ferrara, B. J.; Neal, K.; Bacskai, B. J.; Medarova, Z.; Moore, A. Design, synthesis, and testing of difluoroboron-derivatized curcumins as near-infrared probes for in vivo detection of amyloid-β deposits. *J. Am. Chem. Soc.* **2009**, *131*, 15257−15261.
(9) Schmidt, A.; Pahnke, J. Efficient near-infrared in vivo imaging of amyloid-β deposits in Alzheimer's disease mouse models. *J. Alzheimer's Dis.* **2012**, *30*, 651−664.
(10) Ueno, T.; Nagano, T. Fluorescent probes for sensing and imaging. *Nat. Methods* **2011**, *8*, 642−645.
(11) Raymond, S. B.; Skoch, J.; Hills, I. D.; Nesterov, E. E.; Swager, T. M.; Bacskai, B. J. Smart optical probes for near-infrared fluorescence imaging of Alzheimer's disease pathology. *Eur. J. Nucl. Med. Mol. Imaging* **2008**, *35*, S93−S98.
(12) Li, Q.; Min, J.; Ahn, Y. H.; Namm, J.; Kim, E. M.; Lui, R.; Kim, H. Y.; Ji, Y.; Wu, H.; Wisniewski, T.; Chang, Y. T. Styryl-based compounds as potential *in vivo* imaging agents for beta-amyloid plaques. *ChemBioChem* **2007**, *8*, 1679−1687.
(13) Chung, E.; Prelli, F.; Dealler, S.; Lee, W. S.; Chang, Y. T.; Wisniewski, T. Styryl-based and tricyclic compounds as potential anti-prion agents. *PLoS ONE* **2011**, *6*, 24844.
(14) Ishikawa, K.; Doh-ura, K.; Kudo, Y.; Nishida, N.; Murakami-Kubo, I.; Ando, Y.; Sawada, T.; Iwaki, T. Amyloid imaging probes are useful for detection of prion plaques and treatment of transmissible spongiform encephalopathies. *J. Gen. Virol.* **2004**, *85*, 1785−1790.
(15) Bohrmann, B.; Adrian, M.; Dubochet, J.; Kuner, P.; Muller, F.; Huber, W.; Nordstedt, C.; Dobeli, H. Self-assembly of β-amyloid 42 is retarded by small molecular ligands at the stage of structural intermediates. *J. Struct. Biol.* **2000**, *130*, 232−246.
(16) Yang, Y.; Jia, H. M.; Liu, B. L. (E)-5-styryl-1H-indole and (E)-6-styrylquinoline derivatives serve as probes for β-amyloid plaques. *Molecules* **2012**, *17*, 4252−4265.
(17) Bongarzone, S.; Bolognesi, M. L. The concept of privileged structures in rational drug design: focus on acridine and quinoline scaffolds in neurodegenerative and protozoan diseases. *Expert Opin. Drug Discovery* **2011**, *6*, 251−268.
(18) Sridharan, V.; Avendaño, C.; Menéndez, J. C. Convenient, two-step synthesis of 2-styrylquinolines: an application of the CAN-catalyzed vinylogous type-II Povarov reaction. *Tetrahedron* **2009**, *65*, 2087−2096.
(19) Raymons, S. B.; Kumar, A. T. N.; Boas, D. A.; Bacskai, B. J. Optimal parameters for near infrared fluorescence imaging of amyloid plaques in Alzheimer's disease mouse models. *Phys. Med. Biol.* **2009**, *54*, 6201−6216.
(20) Di, L.; Kerns, E. H.; Fan, K.; McConnell, O. J.; Carter, G. T. High throughput artificial membrane permeability assay for blood−brain barrier. *Eur. J. Med. Chem.* **2003**, *38*, 223−232.
(21) Cavalli, A.; Bolognesi, M. L.; Capsoni, S.; Andrisano, V.; Bartolini, M.; Margotti, E.; Cattaneo, A.; Recanatini, M.; Melchiorre, C. A small molecule targeting the multifactorial nature of Alzheimer's disease. *Angew. Chem. Int. Ed.* **2007**, *46*, 3689−3692.
(22) Yang, F.; Lim, G. P.; Begum, A. N.; Ubeda, O. J.; Simmons, M. R.; Ambegaokar, S. S.; Chen, P. P.; Kayed, R.; Glabe, C. G.; Frautschy, S. A.; Cole, G. M. Curcumin inhibits formation of amyloid beta oligomers and fibrils, binds plaques, and reduces amyloid in vivo. *J. Biol. Chem.* **2005**, *280*, 5892−5901.
(23) Royer, C. A. Probing protein folding and conformational transitions with fluorescence. *Chem. Rev.* **2006**, *106*, 1769−1784.
(24) Groenning, M. Binding mode of Thioflavin T and other molecular probes in the context of amyloid fibrils-current status. *J. Chem. Biol.* **2010**, *3*, 1−18.
(25) Bongarzone, S.; Tran, H. N. A.; Cavalli, A.; Roberti, M.; Carloni, P.; Legname, G.; Bolognesi, M. L. Parallel synthesis, evaluation, and preliminary structure-activity relationship of 2,5-diamino-1,4-benzoquinones as a novel class of bivalent anti-prion compound. *J. Med. Chem.* **2010**, *53*, 8197−8201.
(26) Kuwata, K.; Nishida, N.; Matsumoto, T.; Kamatari, Y. O.; Hosokawa-Muto, J.; Kodama, K.; Nakamura, H. K.; Kimura, K.; Kawasaki, M.; Takakura, Y.; Shirabe, S.; Takata, J.; Kataoka, Y.; Katamine, S. Hot spots in prion protein for pathogenic conversion. *Proc. Natl. Acad. Sci. U.S.A.* **2007**, *104*, 11921−11926.